

1 **Effect of Climate Change and Variability on Extreme** 2 **Rainfall Intensity-Frequency- Duration Relationships: A** 3 **case study of Melbourne**

4
5 **A. G. Yilmaz¹, I. Hossain² and B.J.C. Perera³**

6 [1] Institute of Sustainability and Innovation, College of Engineering and Science, Victoria
7 University, Melbourne, Victoria 8001, Australia.

8 [2] College of Engineering and Science, Victoria University, Melbourne, Victoria 8001,
9 Australia.

10 [3] Institute of Sustainability and Innovation, College of Engineering and Science, Victoria
11 University, Melbourne, Victoria 8001, Australia.

12 Correspondence to: A. G. Yilmaz (Abdullah.yilmaz@vu.edu.au)

13

14 **Abstract**

15 The increased frequency and magnitude of extreme rainfall events due to anthropogenic
16 climate change, and decadal and multi-decadal climate variability question the stationary
17 climate assumption. The possible violation of stationarity in climate can cause erroneous
18 estimation of design rainfalls derived from extreme rainfall frequency analysis. This may
19 result in significant consequences for infrastructure and flood protection projects since design
20 rainfalls are essential input for design of these projects. Therefore, there is a need to conduct
21 frequency analysis of extreme rainfall events in the context of non-stationarity, when non-
22 stationarity is present in extreme rainfall events. A methodology consisting of, threshold
23 selection, extreme rainfall data (peaks over threshold data) construction, trend and non-
24 stationarity analysis, and stationary and non-stationary Generalized Pareto Distribution (GPD)
25 models was developed in this paper to investigate trends and non-stationarity in extreme
26 rainfall events, and potential impacts of climate change and variability on Intensity-
27 Frequency-Duration (IFD) relationships. The developed methodology was successfully
28 implemented using rainfall data from an observation station in Melbourne (Australia) for
29 storm durations ranging from 6 minutes to 72 hours. Although statistically significant trends

1 were detected in extreme rainfall data for storm durations of 30 minute, and 3 and 48 hours,
2 statistical non-stationarity tests and non-stationary GPD models did not indicate non-
3 stationarity for these storm durations and other storm durations. It was also found that the
4 stationary GPD models were capable of fitting extreme rainfall data for all storm durations.
5 Furthermore, the IFD analysis showed that urban flash flood producing hourly rainfall
6 intensities have increased over time.

7 Key words: Climate change, extreme rainfall, peaks over threshold, generalized pareto
8 distribution

9

10 **1 Introduction**

11 Over the last 100 years, global surface temperature has increased approximately by 0.75 °C,
12 and this warming cannot be explained by natural variability alone (IPCC, 2007). IPCC
13 (2007) stated that excessive greenhouse gas emissions due to human activities is the main
14 reason for current global warming. Increasing frequency and magnitude of extreme weather
15 events is one of the main concerns caused by global warming. Increases in extreme rainfall
16 frequency and magnitude have already been recorded in many regions of the world (Mueller
17 and Pfister, 2011; Dourte et al., 2013; Bürger et al., 2014; Jena et al. 2014), even in some
18 regions where the mean rainfall has shown decreasing trends (Tryhlon and DeGaetano, 2011).
19 Moreover, the magnitude and frequency of extreme rainfall events are very likely to increase
20 in the future due to global warming (IPCC, 2007).

21 Increased frequency and magnitude of extreme rainfall events questions the stationary climate
22 assumption (i.e. the statistical properties of the rainfall do not change over time), which is an
23 underlying assumption of frequency analysis of extreme rainfalls. Khaliq et al. (2006)
24 explained that the classical notions of probability of exceedence and return period are no
25 longer valid under non-stationarity. The possible violation of stationarity in climate increases
26 concerns amongst hydrologists and water resources engineers about the accuracy of design
27 rainfalls, which are derived from frequency analysis of extreme rainfall events under the
28 stationary climate assumption. Erroneous selection of design rainfalls can cause significant
29 problems for water infrastructure projects and flood mitigation works, since the design
30 rainfalls are an important input for design of these projects. Therefore, there is a need to
31 conduct frequency analysis of extreme rainfall events under the context of the non-
32 stationarity.

1 Sugahara et al. (2009) carried out a frequency analysis of extreme daily rainfalls in the city of
2 Sao Paulo using data over the period of 1933-2005. They considered non-stationarity in
3 frequency analysis through introducing time dependency to the parameters of Generalized
4 Pareto distribution (GPD), which is one of the widely used distributions in frequency analysis
5 of extreme values. Park et al. (2011) developed non-stationary Generalized Extreme Value
6 (GEV) distribution (another commonly used extreme value distribution) models for frequency
7 analysis of extreme rainfalls in Korea considering non-stationarity similar to Sugahara et al.
8 (2009). Trambly et al. (2013) performed non-stationary heavy rainfall (it should be noted
9 that “heavy” rainfall used here as same as “extreme” rainfall in Sugahara et al. (2009))
10 analysis using daily rainfall data of the period 1958-2008 in France. They incorporated the
11 climatic covariates into the Generalized Pareto Distribution parameters to consider non-
12 stationarity.

13 There are very few studies, which investigated extreme rainfall frequency analysis in the
14 context of non-stationarity in Australia. Jakob et al. (2011a,b) investigated the potential
15 effects of climate change and variability on rainfall intensity-frequency-duration (IFD)
16 relationships in Australia, considering possible non-stationarity of extreme rainfall data in
17 design rainfall estimates. Yilmaz and Perera (2014) developed stationary and non-stationary
18 GEV models using a single station in Melbourne considering data for storm durations ranging
19 from 6 minutes to 72 hours, to construct IFD curves through frequency analysis. They
20 investigated the advantages of non-stationary models over stationary ones using graphical
21 tests.

22 In this paper, it is aimed to investigate extreme rainfall non-stationarity through trend
23 analysis, non-stationarity tests and non-stationary GPD models (NSGPD). The extreme
24 rainfall trend analysis was performed using data from a rainfall station in Melbourne
25 considering storm durations of 6 and 30 minutes, and 1, 2, 3, 6, 12, 24, 48 and 72 hours.
26 Trend analysis was used to determine if the extreme rainfall series have a general increase or
27 decrease over time. However, trends do not necessarily mean non-stationarity. The mean and
28 variance of extreme rainfall data series may not change over time (i.e. stationarity), despite
29 the presence of trends in extreme rainfall data series (Wang et al., 2006). Therefore, further
30 analysis should be conducted to check if the detected trends may correspond to extreme
31 rainfall non-stationarity. Non-stationarity analysis of the extreme rainfall data was further
32 carried out using statistical non-stationarity tests and NSGPD models in this study.

1 Potential effects of climate change on the IFD relationship were investigated through GPD
2 models in this study following the stationarity analysis. Expected rainfall intensities for return
3 periods of 2, 5, 10, 20, 50 and 100 years were derived and compared for two time slices:
4 1925-1966 (i.e. cooler period) and 1967-2010 (warmer period) after selecting 1967 as the
5 change point based on the findings of Yilmaz and Perera (2014). Yilmaz and Perera (2014)
6 conducted the change point analysis for extreme rainfall data for storm durations ranging
7 from 6 minutes to 72 hours in Melbourne, and stated the year 1966 as change point.
8 Moreover, Jones (2012) stated the period 1910-1967 as stationary and 1968-2010 as non-
9 stationary according to the observed minimum and maximum temperature and rainfall data in
10 south eastern Australia (which includes the Melbourne region). Therefore, the entire data set
11 was divided into two periods (i.e. 1925-1966 and 1967-2010) and the IFD information was
12 generated for the two periods to understand if there are any changes in rainfall intensities
13 between these cooler and warmer periods.

14 Changes in rainfall intensities (i.e. IFD information) over time can occur due to both climate
15 change and natural climate modes (i.e. natural climate variability). The ENSO with El Niño
16 and La Niña phases (Verdon et al., 2004), the Indian Ocean Dipole (IOD) (Ashok et al.,
17 2003), the Southern Annual Mode (SAM) (Meneghini et al., 2007), and the Inter-decadal
18 Pacific Oscillation (IPO) (Verdon-Kidd and Kiem, 2009) were expressed as significant
19 climate modes, which have influence on the precipitation variability in Victoria (Australia),
20 which includes the Melbourne region. IPO affects the precipitation variability in Victoria
21 itself; also it modulates the association between ENSO and Australian climate (Power et al.,
22 1999; Kiem et al., 2003; Micevski et al., 2006). ENSO and Australian climate relationship
23 was strong in particular during the IPO negative phases (i.e associated with wetter
24 conditions). Moreover, Kiem et al. (2003) stated that La Niña events, which were increased
25 during the negative IPO phases, are the primary driver for flood risk in Australia. It can be
26 seen from the above studies that there is a need to investigate the IPO and extreme rainfall
27 relationship due to its direct effects on Australian rainfall as well as effects of IPO on ENSO,
28 which has a strong link to Australian rainfall. The effects of IPO on extreme rainfalls were
29 investigated in this study through extreme rainfall IFD analysis during IPO negative and
30 positive phases. Salinger (2005) and Dai (2013) defined time periods of IPO negative and
31 positive phases as 1947-1976 and 1977-1998 respectively. Therefore, extreme rainfall IFD
32 analysis was performed for these two periods to explain the relationship between IPO and
33 extreme rainfalls. It should be noted that potential effects of climate change on design rainfall

1 intensities (IFD information) were investigated through GPD models developed for 1925-
2 1966 and 1967-2010 time periods, whereas IPO and extreme rainfall relationship was
3 investigated with GPD models for the periods of IPO negative (1947-1976) and positive
4 (1977-1998) phases.

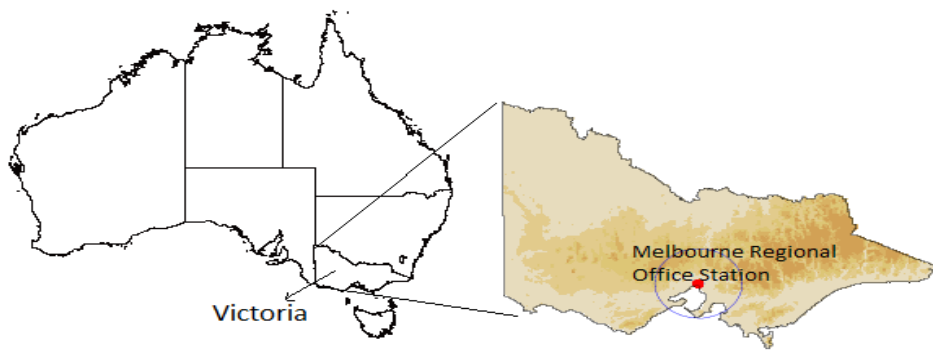
5 As mentioned earlier in this section, there are very limited studies in the literature
6 investigating IFD relationships in Australia considering non-stationarity of extreme rainfall
7 data (e.g. Jakob et al., 2011a,b; Yilmaz and Perera, 2014). However, Jakob et al. (2011 a,b)
8 did not develop non-stationary extreme rainfall models to investigate their performances over
9 stationary models, as it is done in this study. Although, Yilmaz and Perera (2014) developed
10 non-stationary models for the same study area as in this study, they simply used annual
11 maximums as extreme rainfall input to the stationary and non-stationary models. Several
12 studies recommended the use of peaks over threshold (POT) data (derived by selecting values
13 over a certain threshold) instead of annual maximums as extreme rainfall data input to
14 frequency analysis (e.g. Re and Barros, 2009; Trambly et al., 2013), since the POT approach
15 results in larger data sets leading more accurate parameter estimations of extreme value
16 distribution. Therefore, this study used POT data to develop stationary and non-stationary
17 GPD models.

18

19 **2 Study Area and Data**

20 The Melbourne City in Australia was selected as the case study area. Data of the Melbourne
21 Regional Office rainfall station (Site no: 086071; latitude of 37.81 °S and longitude of 144.97
22 °E) were provided by Bureau of Meteorology in Australia. This station was selected for the
23 study, since it has long rainfall records, which are essential for trend and extreme rainfall IFD
24 analysis. Approximate location of the station is shown in Figure 1.

25



1

2 **Figure 1.** Approximate location of the Melbourne Regional Office Rainfall Station

3 Six minute pluviometer data are available from April 1873 to December 2010 at the
4 Melbourne Regional Office station. These data were used to generate rainfall data for storm
5 durations including 30 minute, and 1, 2, 3, 6 and 12 hours. Also, daily rainfall data are
6 available at the Melbourne Regional Office station since April 1855. Daily rainfall data were
7 used to produce 48 and 72 hours rainfall data. Although daily rainfall record is complete,
8 there are missing periods in 6 minute data record. Missing periods in six minute data record
9 were from January 1874 to July 1877 and from July 1914 to December 1924. Therefore,
10 rainfall data over the period 1925-2010 from both sources (i.e. 6 minute and daily) were used
11 for all storm durations in this study.

12

13 **3 Methodology**

14 The methodology of this study consists of the following four steps.

15 (1) Extreme rainfall data were constructed based on the POT approach after selection of
16 suitable thresholds for storms of different durations.

17 (2) Trend analysis of POT data of all storm durations was carried out using non-parametric
18 tests. Then, stationarity analysis was performed for the same data sets using statistical non-
19 stationarity tests and non-stationary GPD models.

20 (3) Stationary GPD models were developed, and design rainfall estimates were derived for
21 standard return periods considering two time slices (1925-1966 and 1967-2010) in order to
22 investigate potential effects of climate change on design rainfall intensities (extreme rainfall
23 IFD information).

1 (4) Stationary GPD models were constructed to obtain design rainfall intensities for IPO
2 negative (1947-1976) and positive (1977-1998) phases to investigate the IPO and extreme
3 rainfall relationship.

5 **3.1 Threshold Selection and Extreme Rainfall Data Set Construction**

6 The first step of the extreme rainfall frequency analysis is to construct the extreme rainfall
7 data set. There are two widely used approaches to construct such data sets: block maxima and
8 peaks over threshold, also called partial duration series approach (Thompson et al., 2009;
9 Lang et al., 1999). In the block maxima approach, a sequence of maximum values is taken
10 from blocks or periods of equal length, such as daily peak rainfall amount over an entire year
11 or season. On the other hand, rainfall values that exceed a certain threshold are selected in the
12 POT approach. Although the block maxima approach is the commonly used method due to
13 its simplicity, it has a very important shortcoming that it uses only one value from each block
14 (Sugahara et al., 2009). This may cause loss of some important information, and also smaller
15 sample sizes, which affect the accuracy of the parameter estimates. Moreover, the POT
16 method has an advantage of investigation of changes in number of events per year as well as
17 magnitude (Jakob et al., 2011a). Due to the above mentioned reasons, the POT approach is
18 recommended for frequency analysis of extreme events (Re and Barros, 2009; Trambly et
19 al., 2013). It should be noted that “extreme rainfall data” and “POT data” terminology has
20 been used interchangeably in the rest of the paper.

21 Despite the above mentioned advantages of the POT method over the block maxima
22 approach, the POT approach is prone to produce dependent data. Data independency is an
23 underlying requirement for use of extreme value distributions in frequency analysis.
24 Therefore, the data dependency was removed in this study from the POT data of all storm
25 durations through the method recommended by Jakob et al. (2011a). They recommended that
26 if there is a cluster of POT events, the POT values 24 hours prior to and after the peak rainfall
27 event, should be removed from the data set. For example, if a peak rainfall value in a cluster
28 of POT data is selected for 9 November 2013, rainfall values over the threshold on 8 and 10
29 November 2013 are not considered in the POT data set. None of the POT data sets (after the
30 application of the method by Jakob et al. (2011a)) showed dependency even at 0.1

1 significance level according to the autocorrelation test as explained in Chiew and Siriwardena
2 (2005).

3 The critical step in the construction of POT data is the selection of the appropriate threshold
4 value. Researchers have proposed several procedures for selecting the thresholds, but a
5 general and objective method is yet to be emerged (Lang et al., 1999; Coles, 2001; Katz et al.,
6 2005). The threshold selection task is a compromise between bias and variance. If the
7 threshold is too low, the asymptotic arguments underlying the derivation of the GPD model
8 are violated. On the other hand, too high threshold will result in fewer excesses (i.e. rainfall
9 values above threshold) to estimate the shape and scale parameter leading to high variance.
10 Therefore, in the threshold selection it should be considered if the limiting model provides a
11 sufficiently good approximation versus the variance of the parameter estimate (Coles, 2001;
12 Katz et al., 2005).

13 Beguería et al. (2011), Coles (2001) and Lang et al. (1999) recommended the mean residual
14 plots to select the threshold. The mean residual plot indicates the relationship between mean
15 excesses (i.e. mean of values above the threshold) and various thresholds. Mean excess is a
16 linear function of threshold in GPD (Coles, 2001). Therefore, threshold value should be
17 selected from the domain, where the mean residual plot shows linearity (i.e. linearity between
18 mean excess and threshold) (Hu, 2013). The exact threshold value can be determined from the
19 linear domain in such a way that on average 1.65 – 3.0 extreme events per year are selected
20 (e.g. Jakob et al., 2011a; Cunnane, 1973). This study adopted the mean residual plot method
21 for selection of appropriate thresholds for all storm durations.

22

23 **3.2 Trend and Non-stationarity Tests**

24 Trends tests can be broadly grouped into two categories: parametric and non-parametric
25 methods. Non-parametric tests are more appropriate for non-normally distributed and
26 censored hydro-meteorological time series data (Bouza-Deano et al., 2008). However, data
27 independency is still a requirement of these tests. Mann-Kendall (MK) and Spearman's rho
28 (SR) are non-parametric rank based trend tests, which are commonly used for trend detection
29 of hydro-meteorological data (Yue et al., 2002). Formulation and details of the MK and SR
30 tests can be found in Kundzewicz and Robson (2000). MK and SR tests were applied to POT

1 data sets of all storm durations (6, 30 minutes, and 1, 2, 3, 6, 12, 24, 48, 72 hours) over the
2 period of 1925-2010 **after applying the autocorrelation test as explained earlier.**

3 Trend tests are used to determine if the time series data has a general increase or decrease in
4 trend. However, increasing or decreasing trends do not guarantee non-stationarity even if they
5 are statistically significant. Therefore, it is useful to conduct further analysis in order to
6 investigate non-stationarity of the data sets. In this study, three statistical tests, namely
7 augmented Dickey-Fuller (ADF), Kwiatkowski–Phillips–Schmidt–Shin (KPSS) and Phillips-
8 Perron (PP), were employed to investigate the non-stationarity in extreme rainfall data. These
9 tests were selected due to their proven capability in hydrological studies (Wang et al., 2005;
10 Wang et al., 2006; Yoo, 2007). Sen and Niedzielski (2010) and van Gelder et al. (2007)
11 explain the details of these tests. Non-stationarity of data is the null hypothesis of ADF and
12 PP tests, whereas the null hypothesis of the KPSS test is stationarity of the data series. Tests
13 were performed at 0.05 significance level in this study. Whenever the significance level is
14 higher than the p-value (probability) of the test statistic, the null hypothesis is rejected.

15

16 **3.3 Stationary GPD Models**

17 Several studies recommended use of GPD for frequency analysis of POT data (e.g. Beguería
18 et al. 2011). Therefore, GPD is used in this study to derive the extreme rainfall IFD
19 relationships. GPD is a flexible, long-tailed distribution defined by shape (γ) and scale (σ)
20 parameters. Eq. (1) shows the cumulative distribution function of GPD. It should be noted
21 that stationary GPD model corresponds to conventional GPD models with constant shape and
22 scale parameters.

$$23 \quad F(y, \sigma, \gamma) = P(X \leq u + y | X \geq u) = \begin{cases} 1 - (1 + \frac{\gamma}{\sigma} y)^{-\frac{1}{\gamma}}, & \sigma > 0, & 1 + \gamma(\frac{y}{\sigma}) > 0 \\ 1 - \exp(\frac{-y}{\sigma}), & \sigma > 0, & \gamma = 0 \end{cases} \quad (1)$$

24 The scale parameter (σ in Eq. (1)) characterizes the spread of distribution, whereas the shape
25 parameter (γ in Eq. (1)) characterizes the tail features (Sugahara et al., 2009). Rainfall
26 intensities in mm/hr for different return periods (2, 5, 10, 20, 50 and 100 years in this study)

1 are calculated using the inverse cumulative distribution function. Details of GPD can be found
2 in Sugahara et al. (2009), Coles (2001) and Rao and Hamed (2000).

3 There are different approaches such as maximum likelihood and L-moments to estimate the
4 parameters of GPD. In this study, the L-moments method was used to estimate GPD
5 parameters since it is less affected by data variability and outliers (Borijeni and Sulaiman,
6 2009). Hosking (1990) described the details of the L-moments method.

7 Goodness of fit of the stationary GPD models was determined using the graphical diagnostics
8 and statistical tests. The probability (P-P) and the quantile (Q-Q) plots are common
9 diagnostic graphs. In P-P plot, the x-axis is empirical cumulative distribution function (CDF)
10 values, whereas the y-axis is theoretical CDF values. In Q-Q plot, the x-axis include input
11 (observed) data values, whereas the y-axis is the theoretical (fitted) distribution quantiles
12 calculated by

$$13 \quad F^{-1}\left(F_n(x_i) - \frac{0.5}{n}\right) \quad (2)$$

14 where $F^{-1}(x)$ is inverse CDF, $F_n(x)$ is empirical CDF, and n is sample size.

15 Close distribution of the points of probability and quantile plots around the unit diagonal
16 indicates a successful fit. Probability and quantile plots explain similar information, however,
17 different pairs of data are used in probability and quantile plots. It is beneficial to use both
18 plots to assess the goodness of fit, since one plot can show a very good fit while the other can
19 show a poor fit. Coles (2001) explains the details of the diagnostic graphs. When probability
20 and quantile plots show different results, statistical tests are useful to determine adequacy of
21 the fit.

22 In addition to diagnostic graphs, Kolmogorov-Smirnov (KS), Anderson-Darling (AD), and
23 Chi-square (CS) statistical tests were used in this study to check the goodness of fit. These
24 tests were used in the past hydrological applications of extreme value analysis (Laio, 2004;
25 Salarpour et al., 2012). They are used to determine if a sample comes from a hypothesized
26 continuous distribution (GPD in this study). Null hypothesis (H_0) of the tests is “data follow
27 the specified distribution”. If the test statistic is larger than the critical value at the specified
28 significance level, then the alternative hypothesis (H_A), which is “data do not follow GPD”, is
29 accepted (Yilmaz and Perera, 2014). Details of these tests can be seen in Di Baldassarre et al.
30 (2009) and Salarpour et al. (2012).

1 As explained in Section 1, the extreme rainfall data of all storm durations were fitted to the
2 stationary GPD models for 1925-1966 and 1967-2010 periods to investigate the climate
3 change effects on IFD information, and for 1947-1976 (IPO negative phase) and 1977-1998
4 (IPO positive phase) to investigate the IPO and extreme rainfall relationship.

5

6 **3.4 Non-stationary GPD (NSGPD) Models**

7 NSGPD models were used along with statistical non-stationarity tests in this study to identify
8 if the detected trends based on MK and SR tests correspond to non-stationarity. If it is proven
9 that extreme rainfall data show non-stationarity over time, it is preferable to use NSGPD
10 models instead of stationary GPD models. Non-stationary GPD models can be developed
11 through the incorporation of non-stationarity feature (i.e. time dependency or climate
12 covariates) into the scale parameter of the stationary GPD model in Eq. (1) (Coles, 2001;
13 Khaliq et al., 2006). Thus, the scale parameter is not constant and varies with time in non-
14 stationary models. It is also possible to incorporate the non-stationarity into the shape
15 parameter. However, it is very difficult to estimate the shape parameter of the extreme values
16 distribution with precision when it is time dependent, and thereby it is not realistic to attempt
17 to estimate the **shape** parameter as a smooth function of time (Coles, 2001).

18 In this study, two types of non-stationary GPD models were developed with parameters as
19 explained below:

- 20 • Model NSGPD1 $\sigma = \exp(\beta_0 + \beta_1 x t), \gamma$ (constant)
- 21 • Model NSGPD2 $\sigma = \exp(\beta_0 + \beta_1 x t + \beta_2 x t^2), \gamma$ (constant)

22 In the above models, β_0, β_1 and β_2 modify the scale parameters of NSGPD models. It should
23 be noted that the exponential function has been adopted to introduce time dependency in the
24 scale parameter to ensure the positivity of scale parameter. **There are other functions, which
25 result in positive scale parameter; however exponential function was used in this study, since
26 it was recommended by some studies (e.g. Furrer et al., 2010) in literature.** NSGPD1 and
27 NSGPD2 were applied to POT data of all storm durations in this study over the two periods
28 (1925-1966 and 1967-2010).

29 The maximum likelihood method was used for parameter estimation of NSGPD models
30 because of its suitability for incorporating non-stationary features into the distribution

1 parameters as covariates (Sugahara et al., 2009). Shang et al. (2011) explain the details of the
2 maximum likelihood method.

3 Superiority of the NSGPD models over the stationary GPD models were investigated through
4 the deviance statistic test. Let M_0 and M_1 be the stationary and the non-stationary models,
5 respectively such that $M_0 \subset M_1$. The deviance test is used to compare the superiority of M_1
6 over M_0 using the log-likelihood difference (D) using the following equation (Coles, 2001, El
7 Adlouni et al., 2007):

$$8 \quad D = 2\{l_1(M_1) - l_0(M_0)\} \quad (3)$$

9 where $l_1(M_1)$ and $l_0(M_0)$ denote the maximised log-likelihood under models M_1 and M_0
10 respectively. The test of the validity of one model against the other (in this case M_1 against
11 M_0) is based on the probability distribution of D , which is approximated by chi-square
12 distribution. For instance, consider comparing NSGPD1 model with three parameters (i.e. β_0 ,
13 β_1, γ) denoted by M_1 in Eq. (3) with stationary GPD model with two constant parameters (i.e.
14 σ and γ) denoted by M_0 in Eq. (3). Under the null hypothesis, the statistic D is approximately
15 chi square distributed with 1 degree of freedom (degree of freedom is decided based on
16 difference between the number of parameters of M_0 and M_1 models). Stationary GPD model
17 (M_0) should be rejected in favor of NSGPD1 (M_1) if $D > c_\alpha$, where c_α is the $(1 - \alpha)$ quantile of
18 a chi square distribution at the significance level of α . Large values of D suggest that model
19 M_1 explains substantially more of the variation in the data than M_0 . More detailed information
20 about deviance statistic test can be found in Coles (2001), Trambly et al. (2013) and
21 Beguer'ia et al. (2011). Superiority of M_1 is an evidence of non-stationarity of extreme
22 rainfall data. In this case, NSGPD models should be used to generate rainfall intensity
23 estimates.

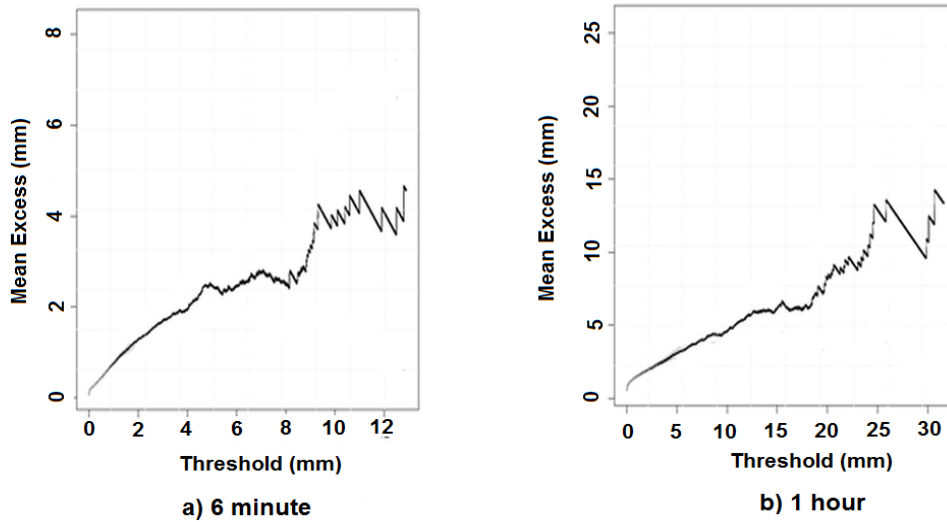
24

25 **4 Results and Discussion**

26 **4.1 Threshold Selection**

27 The thresholds for all storm durations were selected using the mean residual plots based on
28 the linearity of data in these plots as explained in Section 3.1. A range of different threshold
29 values in the linear domain of the mean residual plots were tested to select the final threshold
30 so that the number of extreme rainfall events per year is in the range of 1.65 to 3.0 events

1 (Cunnane, 1973; Jakob et al., 2011a). For example, thresholds of 3.6 mm and 9.8 mm were
 2 selected for 6 minute and 1 hour storm durations respectively using the mean residual plots as
 3 shown in Figure 2. Selected threshold values for all other storm durations are listed in Table
 4 1.



5
 6 **Figure 2.** Mean residual plots for 6 minute and 1 hour storm durations

7
 8 Table 1. Threshold values obtained by using mean residual plot

Storm Duration	Threshold (mm)
6 min	3.6
30 min	8.0
1 hr	9.8
2 hr	15
3 hr	17
6 hr	22
12 hr	25
24 hr	30
48 hr	35
72 hr	40

9

1 **4.2 Trend and Non-stationarity Tests Results**

2 Table 2 summarizes the results of the trend tests. The trend tests (i.e. MK and SR) showed
 3 that extreme rainfall data of 30 minute, 3 and 48 hours exhibited statistically significant
 4 increasing trends at different significance levels. The 30 minute data set showed the most
 5 significant data trend according to both MK and SR tests. It should be noted that only SR test
 6 indicated statistically significant trend for 48 hour data set. Data sets of all other storm
 7 durations except 6 hour also showed increasing trends, however these trends are not
 8 statistically significant even at 0.1 significance level.

9

10 Table 2. Trend analysis results

Storm Durations	Test Statistic		Result
	Mann-Kendal (MK)	Spearman's Rho (SR)	
6 min	0.953	0.99	NS
30 min	2.138 (0.05)	2.052 (0.05)	S (0.05)
1 hr	1.1	1.105	NS
2 hr	1.387	1.333	NS
3 hr	1.674 (0.1)	1.689 (0.1)	S(0.1)
6 hr	-0.058	-0.084	NS
12 hr	0.05	0.046	NS
24 hr	0.587	0.67	NS
48 hr	1.58	1.647 (0.01)	S(0.1)[SR]
72 hr	0.133	0.16	NS

11 Critical values at 0.1, 0.05, and 0.01 significance levels are 1.645, 1.96, and 2.576 respectively.

12 S = statistically significant trends at different significance levels shown within brackets.

13 NS = statistically insignificant trends even at 0.1 significance level.

14 Trends in number of POT events per year were also investigated in this study. It was found
 15 that there is an increasing trend in the number of POT events for storm durations less than or
 16 equal to 2 hours, whereas the number of POT events per year for storm durations greater than
 17 2 hours showed decreasing trends. However, none of these trends were statistically
 18 significant even at 0.1 significance level. Furthermore, the ADF, KPSS and PP non-
 19 stationarity tests did not indicate non-stationarity in any of the extreme rainfall data sets.

1 **4.3 NSGPD Models**

2 Non-stationary models (NSGPD1 and NSGPD2) for all storm durations were developed for
3 1925-1966 and 1967-2010 time slices. The deviance statistic test showed that there was no
4 evidence that any of the non-stationary models outperformed their counterpart stationary
5 models. For example, for the extreme rainfall data set of 3 hour storm duration over period
6 1967-2010, the maximised log-likelihood of stationary GPD model (M_0 in Eq. (3)) is 189.4,
7 whereas the maximised log-likelihood of NSGPD1 and NSGPD2 (M_I in Eq. (3)) are 189.3
8 and 189.1 respectively. D , calculated by Eq. (3), is smaller than c_α for both non-stationary
9 cases (NSGPD1 and NSGPD2). Therefore, it can be stated that non-stationary models do not
10 outperform stationary models for these data sets. This is the case for all other storm durations
11 (including the durations, in which extreme rainfall data showed statistically significant
12 increasing trends) in both time periods (i.e. 1925-1966 and 1967-2010). As explained in
13 Section 4.2, the statistical non-stationarity tests (i.e. ADF, KPSS and PP) also showed that
14 there was no evidence for non-stationarity of extreme rainfall data sets used in this study.
15 Therefore, the stationary GPD models were used for the frequency analysis of extreme
16 rainfall data sets to compare rainfall intensity estimates.

17

18 **4.4 Stationary GPD Models**

19 POT data were used in stationary GPD models for two different pairs of periods:

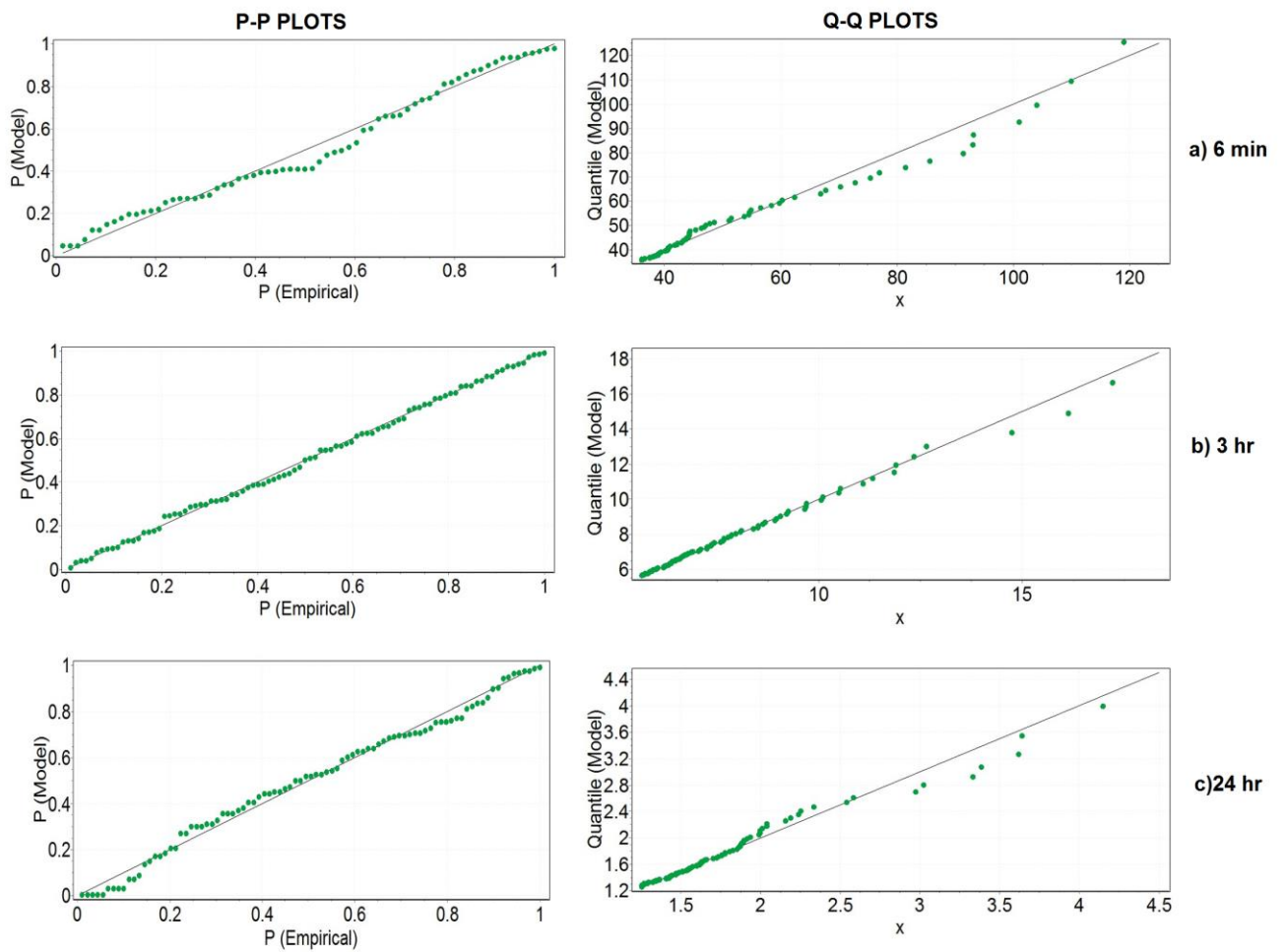
- 20 • 1925-1966 and 1967-2010 (to investigate the effects of climate change),
- 21 • IPO negative (1947-1976) and positive (1977-1998) phases (to investigate the IPO and
22 extreme rainfall relationship),

23 to compute IFD information under stationary conditions.

24 This section explains the results of stationary GPD models over 1925-1966 and 1967-2010
25 periods, whereas Section 4.5 shows the results of GPD models developed for the IPO
26 analysis.

27 The graphical diagnostic and statistical tests showed that all extreme data sets (for all storm
28 durations) were successfully fitted with the stationary GPD models. As examples, Figure 3
29 shows the diagnostic graphs (i.e. probability and quantile plots) of stationary GPD models for
30 the extreme rainfall data of 6 minute, and 3 and 24 hours storm durations over the 1925-1966

1 period. Table 3 indicates the results of the stationary GPD analysis (i.e. rainfall intensity
 2 estimates), whereas Figure 4 illustrates the same information graphically for all storm
 3 durations.



4
 5 **Figure 3.** Goodness of fit for extreme rainfall data of 6 minute, 3 hour and 24 hour over 1925-
 6 1966 period

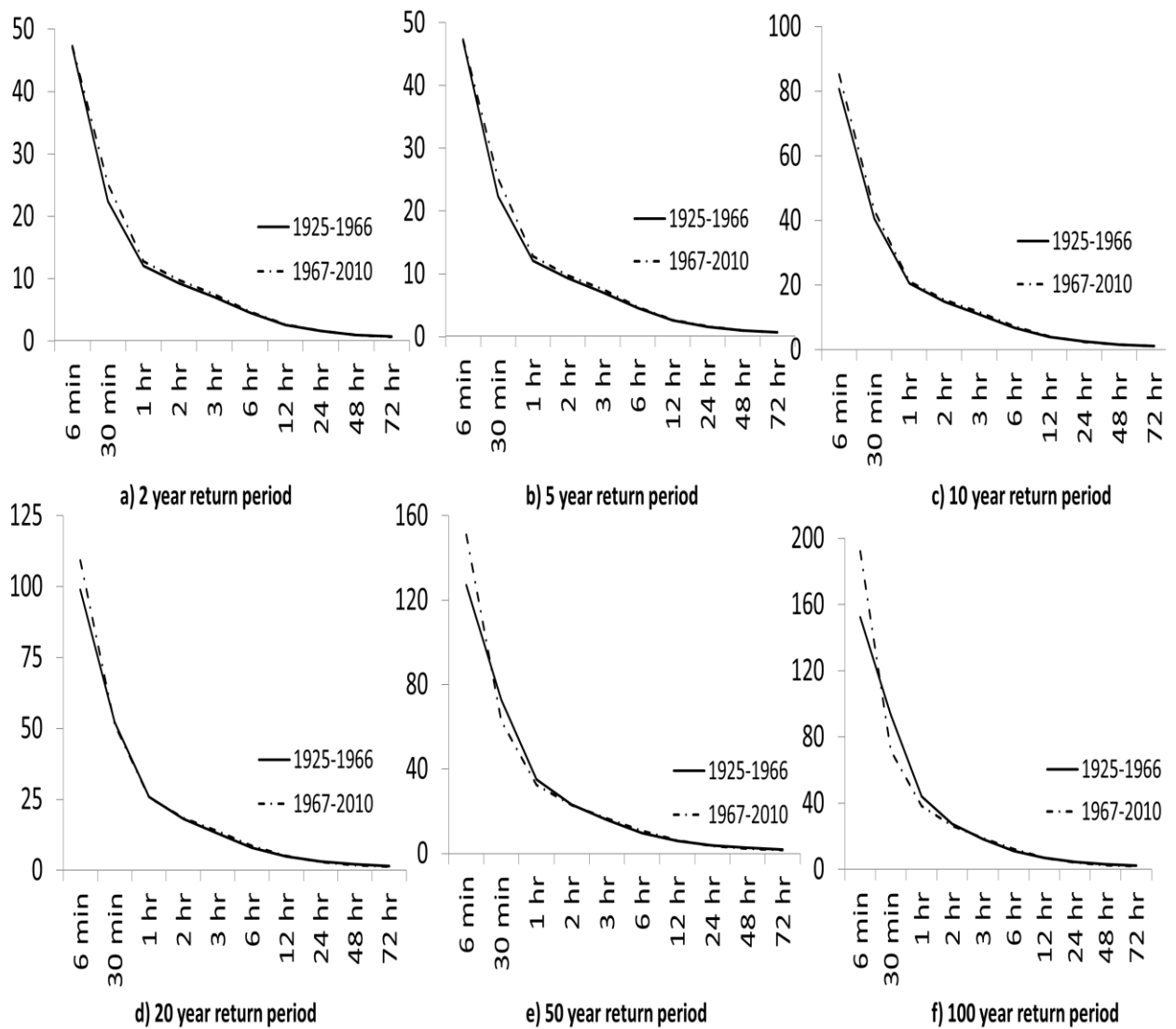
7
 8
 9
 10
 11
 12

1 Table 3. Rainfall intensity (mm/hr) estimates derived from stationary GPD models over
 2 periods 1925-1966 and 1967-2010

Durations/Return Period	2 year		5 year		10 year	
	1925-1966	1967-2010	1925-1966	1967-2010	1925-1966	1967-2010
6 min	47.1	47.3	64.9	66.4	80.7	85.3
30 min	22.4	25.2	31.5	35.2	40.6	43.2
1 hr	12.1	12.8	16.4	17.3	20.6	21.2
2 hr	9.3	9.8	12.3	12.9	15.0	15.5
3 hr	7.1	7.5	9.2	9.8	10.9	11.7
6 hr	4.5	4.7	5.8	6.1	6.8	7.3
12 hr	2.5	2.6	3.4	3.5	4.1	4.2
24 hr	1.6	1.6	2.2	2.1	2.6	2.5
48 hr	1.0	0.9	1.4	1.3	1.7	1.6
72 hr	0.8	0.7	1.0	0.9	1.2	1.1

Durations/Return Period	20 year		50 year		100 year	
	1925-1966	1967-2010	1925-1966	1967-2010	1925-1966	1967-2010
6 min	98.9	109.2	127.1	150.9	152.2	192.2
30 min	52.2	51.4	72.8	62.8	93.5	71.8
1 hr	25.9	25.7	35.1	32.4	44.2	38.2
2 hr	18.1	18.5	23.1	22.8	27.5	26.5
3 hr	12.9	13.7	15.9	16.6	18.5	19.0
6 hr	8.0	8.7	9.8	10.7	11.2	12.4
12 hr	4.8	5.0	6.0	6.1	6.9	7.1
24 hr	3.1	3.0	3.8	3.6	4.5	4.1
48 hr	2.1	1.9	2.7	2.3	3.2	2.7
72 hr	1.5	1.4	2.0	1.8	2.4	2.1

3



1

2 **Figure 4.** Rainfall intensity estimates from stationary GPD models

3

4 Primary findings of the stationary GPD analysis are listed below:

5 - Rainfall intensity estimates of the stationary GPD models over the period 1925-1966
 6 were larger than those estimates of the period 1967-2010 for all storm durations equal or
 7 greater than 24 hours (i.e. 24, 48 and 72 hours) except 24 hour storm duration of 2 year return
 8 period.

9 - For return periods less than or equal to 10 years, rainfall intensity estimates of sub-
 10 daily storm durations for the period of 1967-2010 were larger than those estimates of the
 11 1925-1966 period.

1 - For the return periods above 10 year, majority of hourly rainfall intensity estimates
2 over the period 1967-2010 were larger than those estimates for the period of 1925-1966.

3 It is possible to conclude then that urban flash flood (i.e. flooding occurring in less than 6
4 hours of rain (Hapuarachchi et al., 2011)) producing hourly rainfall intensities have increased
5 over time (i.e. from 1925-1966 to 1967-2010) with minor exceptions (i.e. 1 hour storm
6 durations of return periods above 10 years, and 2 hour storm duration of 50 and 100 year
7 return periods). It should be noted that 90% confidence limits of rainfall intensity estimates
8 were also calculated, but they are not shown in Figure 4 to remove the clutter in the plots.

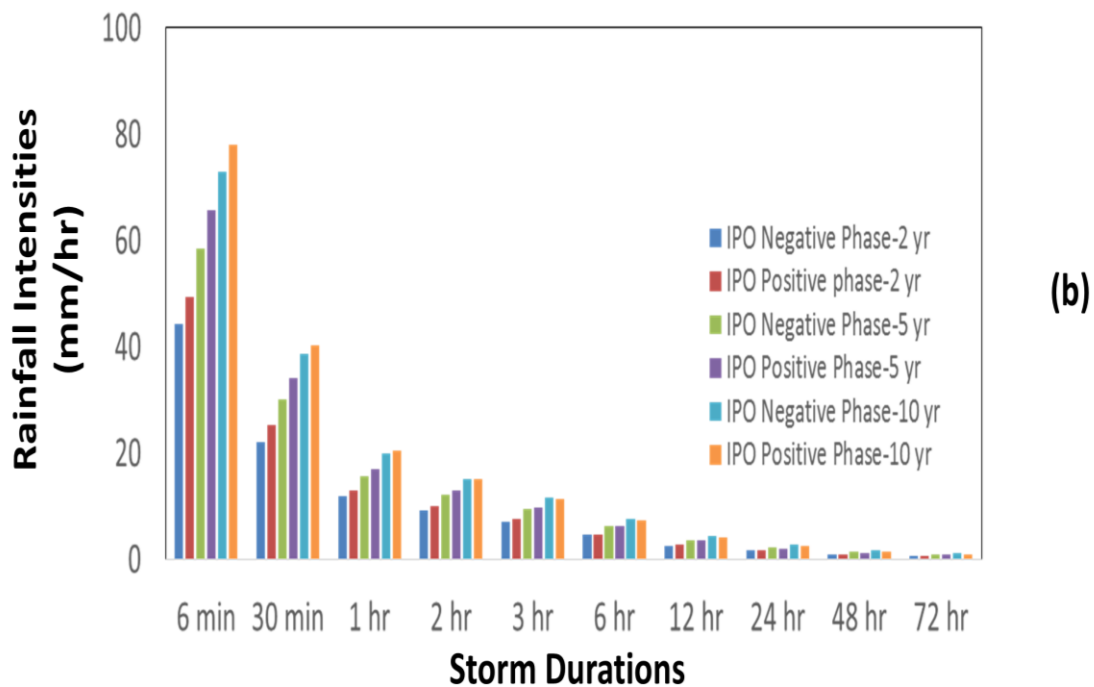
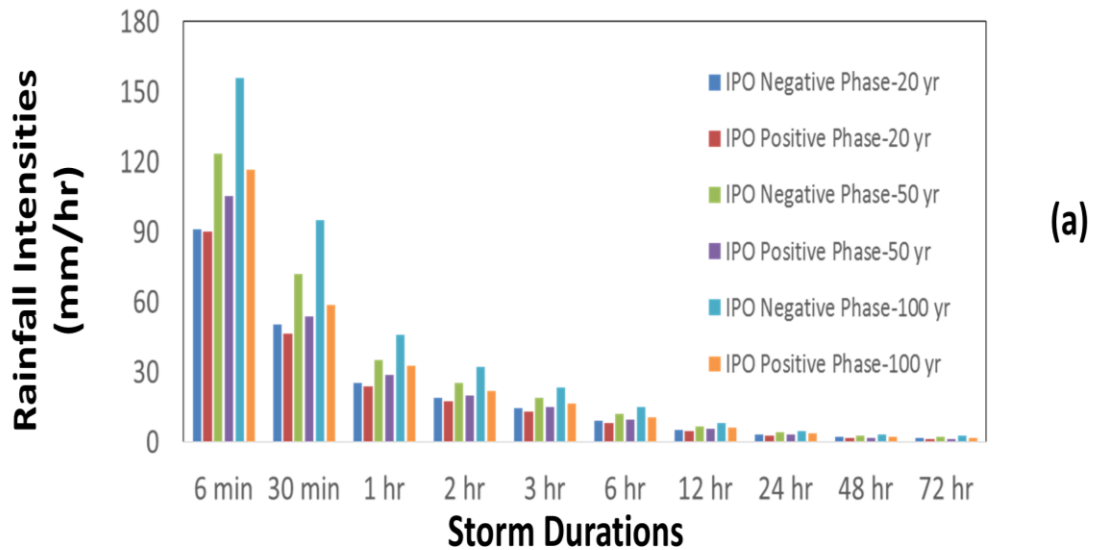
10 **4.5 IPO Analysis**

11 The relationship between extreme rainfall data and IPO was investigated through IFD analysis
12 for the periods of IPO negative (1947-1976) and positive (1977-1998) phases. Results of the
13 IPO analysis are shown in Table 4 and Figure 5.

1 Table 4. Rainfall intensity (mm/hr) estimates derived from IPO Analysis

Durations/ Return Periods	2 year		5 year		10 year	
	IPO Negative Phase	IPO Positive Phase	IPO Negative Phase	IPO Positive Phase	IPO Negative Phase	IPO Positive Phase
6 min	44.2	49.3	58.6	65.8	73.0	78.0
30 min	22.2	25.4	30.2	34.1	38.7	40.3
1 hr	11.9	12.8	15.7	17.1	19.8	20.5
2 hr	9.1	9.9	12.1	12.9	15.0	15.1
3 hr	7.2	7.6	9.5	9.7	11.7	11.3
6 hr	4.7	4.8	6.1	6.2	7.6	7.3
12 hr	2.6	2.7	3.5	3.6	4.3	4.2
24 hr	1.7	1.6	2.2	2.1	2.7	2.4
48 hr	1.0	0.9	1.4	1.2	1.8	1.5
72 hr	0.8	0.7	1.0	0.9	1.3	1.0
Durations/ Return Periods	20 year		50 year		100 year	
	IPO Negative Phase	IPO Positive Phase	IPO Negative Phase	IPO Positive Phase	IPO Negative Phase	IPO Positive Phase
6 min	91.3	89.9	123.5	105.3	155.7	116.6
30 min	50.3	46.3	71.9	53.6	94.9	58.9
1 hr	25.3	24.0	35.4	28.8	46.0	32.7
2 hr	18.9	17.2	25.5	20.0	32.0	22.0
3 hr	14.3	12.9	18.9	14.9	23.2	16.3
6 hr	9.3	8.3	12.2	9.7	14.9	10.6
12 hr	5.3	4.8	6.9	5.6	8.4	6.2
24 hr	3.3	2.7	4.1	3.2	4.8	3.5
48 hr	2.2	1.7	2.8	2.0	3.3	2.2
72 hr	1.6	1.2	2.1	1.4	2.5	1.6

2



1

2 **Figure 5.** Graphical illustration of results of IPO negative and positive phase analysis

3

4 Results of the IPO analysis (Table 4 and Figure 5) can be summarized as follows:

5 -The rainfall intensities of storm durations equal to or greater than 24 hours (24, 48
 6 and 72 hours) for all return periods during the IPO negative phase were larger than the
 7 corresponding rainfall intensities during the IPO positive phase.

8 -The rainfall intensities of all storm durations for the return periods greater than or
 9 equal to 20 years (i.e. 20, 50 and 100 years) during the IPO negative phase exhibited larger

1 values relative to those rainfall intensities for the IPO positive phase as can be seen Table 4
2 and Figure 5 (a).

3 -Rainfall intensities of storm durations below 3 hours for the return periods less than
4 or equal to 10 years (i.e. 2, 5 and 10 years) during the IPO negative phase were lower than
5 those design rainfall intensities for the positive phase. This was also the case for the rainfall
6 intensity estimates for storm durations between 3 and 12 hours for return periods of 2 and 5
7 years.

8 In summary, increases in rainfall intensities were observed during the IPO negative phase for
9 storms with long durations and high return periods, which are consistent with the literature
10 (Kiem et al., 2003). In other words, the IPO negative phase can be the driver for higher
11 rainfall intensities for long durations and high return periods. However, the trends in extreme
12 rainfall data and differences in rainfall intensities for short storm durations and return periods
13 cannot be explained with the IPO influence.

14 In this study, only the relationship of IPO and extreme rainfall was investigated since the
15 literature indicated IPO as very influential climate mode on extreme rainfall events in
16 Victoria. However, there is a need to examine relationships between extreme rainfalls and
17 other climate modes to correctly identify the primary driver for the extreme rainfall trends and
18 differences in rainfall intensity estimates. Also, it is necessary to conduct similar analysis
19 using data of other stations to assess the findings of this study.

20

21 **4.6 Climate Change and Extreme Rainfalls**

22 Anthropogenic climate change may be the reason for the findings of this study (differences in
23 rainfall intensity estimates over time and detected trends). Anthropogenic climate change can
24 impact not only the extreme rainfalls directly, but also the dynamics of key climate modes.
25 **Climate change causes increases in intensity and frequency of extreme rainfalls, since
26 atmosphere can hold more water vapour in a warmer climate (Chu et al. 2013). Increase in
27 rainfall extremes is larger than changes in mean rainfall in a warmer climate, because extreme
28 precipitation relates to increases in moisture content of atmosphere (Kharin and Zwier 2005).**

29 Some studies (e.g. Murphy and Timbal, 2008; CSIRO, 2010) on rainfall changes in south
30 eastern Australia stated that although there is no clear evidence to attribute rainfall change

1 directly to the anthropogenic climate change, it still cannot be ignored. Rainfall changes are
2 linked at least in part to the climate change in south eastern Australia. Nevertheless, it is very
3 difficult to attribute extreme rainfall trends and rainfall intensity differences to anthropogenic
4 climate change due to the limited historical data records and strong effects of natural climate
5 variability (Westra et al., 2010). Further analysis to investigate the reasons of the extreme
6 rainfall trends and design rainfall intensity differences is beyond the scope of this paper.

7

8 **5 Conclusions**

9 A methodology consisting of, threshold selection, extreme rainfall data (peaks over threshold
10 data) construction, trend and non-stationarity tests, and stationary and non-stationary
11 Generalized Pareto Distribution (GPD) models was developed in this paper to investigate the
12 potential effects of climate change and variability on extreme rainfalls and Intensity-
13 Frequency-Duration (IFD) relationships. The developed methodology was successfully
14 implemented using extreme rainfall data of a single observation station in Melbourne
15 (Australia). Same methodology can be adopted for other stations in order to develop larger
16 spatial scale studies by analysing data of multiple stations. Major findings and conclusions of
17 this study are as follows:

18 - Statistically significant extreme rainfall (in mm) trends were detected for storm
19 durations of 30 minute, 3 and 48 hours, considering the data from 1925 to 2010.

20 - **Statistically insignificant increasing trends in the number of POT events were found**
21 **for storm durations less than or equal to 2 hours, whereas statistically insignificant decreasing**
22 **trends were detected in the number of POT events per year for storm durations greater than 2**
23 **hours.**

24 - Despite to the presence of trends in extreme rainfall data for above storm durations
25 **(i.e. 30 minute, 3 and 48 hours)**, there was no evidence of non-stationarity according to
26 statistical non-stationarity tests and non-stationary GPD models. The developed non-
27 stationary GPD models did not show any advantage over the stationary models.

28 - The stationary GPD models were capable of fitting extreme rainfall data for all storm
29 durations **according to the graphical and statistical tests.**

30 - Urban flash flood producing hourly rainfall intensities have increased between the
31 time periods 1925-1966 and 1967-2010.

1 - Analysis on relationship between the Inter-decadal Pacific Oscillation (IPO) and
2 extreme rainfalls showed that the IPO can be responsible for higher rainfall intensities for
3 long durations and high return periods. On the other hand, the IPO cannot be shown as a
4 driver for the trends in extreme rainfall data and differences in rainfall intensities for short
5 storm durations and return periods.

6
7 It should be noted that this study used data from a single station to demonstrate the
8 methodology for future studies. It is not realistic to extrapolate the findings of this study for
9 larger spatial scales such as even the entire Melbourne metropolitan area without further
10 analysis using rainfall data from multiple observation stations within the area. It is
11 recommended applying the methodology developed in this study using data from multiple
12 stations for larger spatial scales. It is also recommended conducting similar analysis of this
13 study for future time periods using future rainfall data derived from climate models, since
14 several studies highlighted very likely increases in intensity and frequency of extreme
15 rainfalls in future.

16 17 **References**

18 Ashok, K., Guan, Z., and Yamagata, T.: Influence of the Indian Ocean Dipole on the
19 Australian winter rainfall, *Geophysical Research Letters*, 30, doi: 10.1029/2003GL017926,
20 2003.

21 Beguería, S., Angulo-Martinez, M., Vicente-Serrano, S.M., Lopez-Moreno, J.I., and El-
22 Kenawy, A.: Assessing trends in extreme precipitation events intensity and magnitude using
23 non-stationary peaks-over-threshold analysis: a case study in northeast Spain from 1930 to
24 2006. *International Journal of Climatology*, 31, 2102–2114, 2011.

25 Borujeni, S.C., and Sulaiman, W.N.A.: Development of L-moment based models for extreme
26 flood events. *Malaysian Journal of Mathematical Sciences*, 3, 281-296, 2009.

27 Bouza-Deano, R., Ternero-Rodriguez, M., and Fernandez-Espinosa, A.J.: Trend study and
28 assessment of surface water quality in the Ebro River (Spain), *Journal of Hydrology*, 361,
29 227-239, 2008.

1 Bürger, G., Heistermann, M., and Bronstert, A.: Towards Subdaily Rainfall Disaggregation
2 via Clausius–Clapeyron, *Journal of Hydrometeorology*, 15, 1303–1311,
3 doi: <http://dx.doi.org/10.1175/JHM-D-13-0161.1>, 2014.

4 Chiew, F., and Siriwardena, L.: *Trend. CRC for Catchment Hydrology: Australia*, 29, 2005.

5 Chu, P.-S., Chen, D.-J., Lin, P.-L.: Trends in precipitation extremes during the typhoon
6 season in Taiwan over the last 60 years. *Atmospheric Science Letters*, 15: 37–43, doi:
7 [10.1002/asl2.464](https://doi.org/10.1002/asl2.464), 2014.

8 Coles S. 2001. *An Introduction to Statistical Modeling of Extreme Values*. Springer-Verlag
9 Inc.: London, UK; 208.

10 CSIRO, *Climate variability and change in south-eastern Australia: A synthesis of findings*
11 *from Phase 1 of the South Eastern Australian Climate Initiative (SEACI)*, Sydney, Australia,
12 2010.

13 Cunnane, C.: A particular comparison of annual maxima and partial duration series methods
14 of flood frequency prediction, *Journal of Hydrology*, 18, 257–271, 1973.

15 Dai, A.: The influence of the inter-decadal Pacific oscillation on US precipitation during
16 1923–2010, *Climate Dynamics*, 41, 633-646, 2013.

17 Di Baldassarre, G., Laio, F., and Montanari, A.: Design flood estimation using model
18 selection criteria, *Physics and Chemistry of the Earth*, 34, 606–611, 2009.

19 Dourte, D., Shukla, S., Singh, P., and Haman, D.: Rainfall Intensity-Duration-Frequency
20 Relationships for Andhra Pradesh, India: Changing Rainfall Patterns and Implications for
21 Runoff and Groundwater Recharge, *Journal of Hydrologic Engineering*, 18(3), 324–330,
22 2013.

23 El Adlouni, S., Ouarda, T.B.M.J., Zhang, X., Roy, R., and Bobée, B.: Generalized maximum
24 likelihood estimators for the nonstationary generalized extreme value model, *Water*
25 *Resources Research*, 43, 2007.

26 Furrer, E.M., Katz, R.W., Walter, M.D., and Furrer, R.: Statistical modeling of hot spells and
27 heat waves, *Climate Research*, 43, 191-205, doi: [10.3354/cr00924](https://doi.org/10.3354/cr00924), 2010.

28 Hapuarachchi, H.A.P., Wang, Q.J., and Pagano, T.C.: A review of advances in flash flood
29 forecasting, *Hydrological Processes*, 25, 2771–2784, DOI: [10.1002/hyp.8040](https://doi.org/10.1002/hyp.8040), 2011.

- 1 Hosking, J.R.M.: L-moments: analysis and estimation of distributions using linear
2 combinations of order statistics, *Journal of the Royal Statistical Society Series B*, 52, 105–
3 124, 1990.
- 4 Hu, Y. 2013. *Extreme Value Mixture Modelling with Simulation Study and Applications in*
5 *Finance and Insurance*, University of Canterbury, New Zealand, 115.
- 6 IPCC: *Climate Change 2007: The Physical Science Basis, Contribution of Working Group I*
7 *to the Fourth Assessment Report of the Intergovernmental Panel on Climate Change.*” edited
8 by:Solomon, S., Qin, D., Manning, M., Chen, Z., Marquis, M., Averyt, K. B., Tignor, M., and
9 Miller, H. L., Cambridge, United Kingdom and New York, USA, 996, 2007.
- 10 Jakob, D., Karoly, D.J., and Seed, A. (a): Non-stationarity in daily and sub-daily intense
11 rainfall – Part 1: Sydney, Australia, *Natural Hazards and Earth System Sciences*, 11, 2263–
12 2271, 2011a.
- 13 Jakob, D., Karoly, D.J., and Seed, A. (b): Non-stationarity in daily and sub-daily intense
14 rainfall – Part 2: Regional Assessment for sites in south-east Australia, *Natural Hazards and*
15 *Earth System Sciences*, 11, 2273–2284, 2011b.
- 16 Jena, P.P, Chatterjee, C., Pradhan, G., and Mishra, A.: *Are recent frequent high floods in*
17 *Mahanadi basin in eastern India due to increase in extreme rainfalls?*, *Journal of Hydrology*,
18 *517, 847-862, 2014.*
- 19 Jones, R.N.: Detecting and Attributing Nonlinear Anthropogenic Regional Warming in
20 Southeastern Australia, *Journal of Geophysical Research*, 117, doi:10.1029/2011JD016328,
21 2012.
- 22 Katz, R.W., Brush, G.S., and Parlange, M.B.: Statistics of extremes modeling ecological
23 disturbances, *Ecology*, 86, 1124–1134, 2005.
- 24 Khaliq, M.N., Ouarda, T.B.M.J., Ondo, J-C., Gachon, P., and Bobee, B.: Frequency analysis
25 of a sequence of dependent and/or non-stationary hydro-meteorological observations: A
26 review, *Journal of Hydrology*, 329, 534-552, 2006.
- 27 Kharin, V. V., and F. W. Zwiers: *Estimating extremes in transient climate change simulations.*
28 *Journal of Climate*, 18, 1156-1173, 2005.

1 Kundzewicz, Z.W., and Robson, A.: Detecting trend and other changes in hydrological data.
2 WCDMP, no. 45; WMO-TD, no. 1013, World Meteorological Organization, Geneva,
3 Switzerland, 2000.

4 Kiem, A.S., Franks, S.W., and Kuczera, G.: Multi-decadal variability of flood risk,
5 Geophysical Research Letters, 30, 1035, 2003.

6 Laio, F.: Cramer–von Mises and Anderson-Darling goodness of fit tests for extreme value
7 distributions with unknown parameters, Water Resources Research, 40, W09308,
8 doi:10.1029/2004WR003204, 2004.

9 Lang, M., Ouarda, T.B.M.J., and Bobee, B.: Towards operational guidelines for over-
10 threshold modelling, Journal of Hydrology, 225, 103–117, 1999.

11 Meneghini, B., Simmonds, I., and Smith, I.N.: Association between Australian rainfall and
12 the Southern Annular Mode, International Journal of Climatology, 27, 109–121, 2007.

13 Micevski, T., Franks, S.W., and Kuczera, K.: Multidecadal variability in coastal eastern
14 Australian flood data, Journal of Hydrology, 327, 219–225, 2006.

15 **Mueller, E.N., and Pfister, A.: Increasing occurrence of high-intensity rainstorm events**
16 **relevant for the generation of soil erosion in a temperate lowland region in Central Europe,**
17 **Journal of Hydrology, 411, 266–278, 2011.**

18 Murphy, B.F., and Timbal, B.: A review of recent climate variability and climate change in
19 southeastern Australia, International Journal of Climatology, 28, 859–879, 2008.

20 Park, J-S., Kang, H-S., Lee, Y.S., and Kim, M-K.: Changes in the extreme daily rainfall in
21 South Korea, International Journal of Climatology, 31, 2290–2299, 2011.

22 Power, S., Casey, T., Folland, C., Colman, A., and Mehta, V.: Interdecadal modulation of the
23 impact of ENSO on Australia, Climate Dynamics, 15, 319–324, 1999.

24 Rao, A.R., and Hamed, K.H.: Flood frequency analysis. CRC, Boca Raton, FL, 2000.

25 Re, M., and Barros, V.R.: Extreme rainfalls in SE South America, Climatic Change, 96, 119–
26 136, 2009.

27 Salarpour, M., Yusop, Z., and Yusof, F.: Modeling the Distributions of Flood Characteristics
28 for a Tropical River Basin, Journal of Environmental Science and Technology, 5, 419–429,
29 2012.

1 Salinger, M.J.: Climate variability and change: past, present and future – an overview,
2 *Climatic Change*, 70, 9–29, 2005.

3 Sen, A.K., and Niedzielski, T.: Statistical Characteristics of River flow Variability in the Odra
4 River Basin, Southwestern Poland, *Polish Journal of Environmental Studies*, 19, 387-397,
5 2010.

6 Shang, H., Yan, J., Gebremichael, M., and Ayalew, S.M.: Trend analysis of extreme
7 precipitation in the Northwestern Highlands of Ethiopia with a case study of Debre Markos,
8 *Hydrology and Earth System Sciences*, 15, 1937–1944, 2011.

9 Sugahara, S., da Rocha, R.P., and Silveira, R.: Non-stationary frequency analysis of extreme
10 daily rainfall in Sao Paulo, Brazil, *International Journal of Climatology*, 29, 1339-1349, 2009.

11 Thompson, P., Cai, Y., Reeve, D., and Stander, J.: Automated threshold selection methods for
12 extreme wave analysis, *Coastal Engineering*, 56, 1013-1021, 2009.

13 Trambly, Y., Neppel, L., Carreau, J., and Najib, K.: Non-stationary frequency analysis of
14 heavy rainfall events in southern France, *Hydrological Sciences Journal*, 58, 280-194, 2013.

15 Tryhorn, L., and DeGaetano, A.: A comparison of techniques for downscaling extreme
16 precipitation over the Northeastern United States, *International Journal of Climatology*, 31,
17 1975-1989, 2011.

18 van Gelder, P.H.A.J.M., Wang, W., and Vrijling, J.K.: Statistical Estimation Methods for
19 Extreme Hydrological Events, *Extreme Hydrological Events: New Concepts for Security*,
20 O.F. Vasiliev et al. (eds.), 199–252, 2007.

21 Verdon, D.C., Wyatt, A.M., Kiem, A.S., and Franks, S.W.: Multi-decadal variability of
22 rainfall and streamflow– Eastern Australia. *Water Resources Research* 40:
23 W10201, doi:10.11029/12004WR003234, 2004.

24 Verdon-Kidd, D.C., and Kiem, A.S.: On the relationship between large-scale climate modes
25 and regional synoptic patterns that drive Victorian rainfall, *Hydrology Earth System Sciences*,
26 13, 467–479, 2009.

27 Wang, W., Van Gelder, P.H.A.J.M., and Vrijling, J.K.: Trend and Stationarity Analysis for
28 Streamflow Processes of Rivers in Western Europe in the 20th Century. IWA International
29 Conference on Water Economics, Statistics, and Finance, Rethymno, Greece, 8-10 July 2005.

1 Wang, W., Vrijling, J.K., Van Gelder, P.H.A.J.M., and Mac, J.: Testing for nonlinearity of
2 streamflow processes at different timescales, *Journal of Hydrology*, 322, 247-268, 2006.

3 Westra, S., Varley, I., Jordan, P., Nathan, R., Ladson, A., Sharma, A., and Hill, P.:
4 Addressing climate non-stationarity in the assessment of flood risk. *Australian Journal of*
5 *Water Resources*,14, 1-16, 2010.

6 Yilmaz, A.G., and Perera, B.J.C.: Extreme Rainfall Non-stationarity Investigation and
7 Intensity-Frequency-Duration Relationship, *Journal of Hydrologic Engineering*
8 10.1061/(ASCE)HE.1943-5584.0000878 (online July 8, 2013), 2013.

9 Yoo, S-H.: Urban Water Consumption and Regional Economic Growth: The Case of Taejeon,
10 Korea, *Water Resources Management*, 21, 1353–1361, 2007.

11 Yue, S., Pilon, P., Cavadias, G.: Power of the Mann Kendall and Spearman’s rho tests for
12 detecting monotonic trends in hydrological series, *Journal of Hydrology*, 259, 254-271, 2002.

13
14
15
16
17
18
19
20
21
22
23
24
25